J Bionic Eng 16 (2019) 608–620
DOI: https://doi.org/10.1007/s42235-019-0049-9

Journal of Bionic Engineering
http://www.springer.com/journal/42235

Improving Kinematic Flexibility and Walking Performance of a Six-legged Robot by Rationally Designing Leg Morphology

Jie Chen[1], Zhongchao Liang[1*], Yanhe Zhu[2*], Jie Zhao[2]

1. *School of Mechanical Engineering and Automation*, *Northeastern University*, *Shenyang* 110819, *China*
2. *State Key Laboratory of Robotics and System*, *Harbin Institute of Technology*, *Harbin* 150001, *China*

Abstract

This paper explores the design of leg morphology in a six-legged robot. Inspired by nature, where animals have different leg morphology, we examined how the difference in leg morphology influences behaviors of the robot. To this end, a systematic search was conducted by scanning over the parameter space consisting of default angles of leg joints of the six-legged robot, with two main objectives: to maximize the kinematic flexibility and walking performance of the robot. Results show that (1) to have a high kinematic flexibility with both the torso and swing legs, the femur segment should tilt downwards by 5° – 10° and the tibia segment should be vertically downwards or with a slight inward tilt; (2) to achieve relatively energy-efficient and steady walking, the tibia segment should be approximately vertically downwards, with the femur segment tilting upwards to lower the torso height. The results of this study suggest that behaviors of legged robots can be passively enhanced by careful mechanical design choices, thereby leading to more competent legged machines.

Keywords: six-legged robot, leg morphology, kinematic flexibility, walking performance

1 Introduction

Legged robots have been among the most active areas in robotic research over the last few decades[1–3]. To date, a variety of legged machines have been constructed, where a range of related techniques both in the field of hardware design and control schemes were involved and reported. Despite remarkable progress, there are still multiple issues remaining to be addressed further, among which determining proper leg morphology (*i.e.* default kinematic configuration of a leg) for a legged robot is one of the most intractable.

Nature has been always an important source of inspiration for scientists and engineers to design and develop legged machines[4,5]. A representative example is the addition of various forms of elastic elements in robotic legs, which takes inspiration from musculoskeletal structures of biological systems[6–9]. These bio-inspired designs have increased the performance of legged robots, and meanwhile advanced our understanding towards biological mechanisms. However, for the design of leg morphology of legged robots, it seems challenging to straightforwardly utilize nature's solutions. One reason is that nature exhibits not just one option for a particular case. A relevant example is that, the bending directions of ostrich and human legs are exactly opposite despite their similar anatomical structure[10–12]. Another reason for this challenge is that modifications are often made during the transfer of biological legs to robotic ones, for the sake of engineering purpose. For instance, legs of multi-legged robots are probably designed identical for ease of technical realization and maintenance, whereas their biological counterparts usually have different forelegs and hindlegs[13–15]. Under these circumstances, further investigations have to be carried out to search for possible design clues.

So far, a series of studies have been conducted to explore the possible influences of leg morphology. For example, Haberland *et al.*[10] investigated the inherent effect of knee joint bending direction on running efficiency of bipedal robots. It is found that bipedal robots with backwards knees exhibited a strong tendency to be more efficient than those with forward knees. The authors pointed out such energetic benefit are mainly resulted from the lower torque and reduced motion at the hip when with backwards knees. Likewise, Smith *et*

***Corresponding author:** Zhongchao Liang, Yanhe Zhu
E-mail: liangzc@me.neu.edu.cn, yhzhu@hit.edu.cn

al.[16] investigated the influence of knee joint bending direction of hindlegs, by using a canine-inspired quadrupedal robot. They found that the bending backwards knees are able to produce more efficient and faster locomotion. It is concluded that simply copying from nature may not lead to optimal performance. Apart from Ref. [16], a series of theoretical and simulation studies have been conducted and suggested that the configuration of foreleg bending backwards and hindleg bending forwards is more advantageous for quadruped robots[17–19]. These studies argued that such configuration is more advantageous over others in terms of overcoming foot slippage and torso pitch oscillation. All these attempts have demonstrated the effectiveness of appropriately designing leg morphology to enhance locomotion behaviors.

Despite the existing research work and publications, the basic role of leg morphology in legged robots is still not fully explored, largely due to the diversity of configurations and designs of legged systems. With this fact in mind, this paper attempts to further investigate the design of leg morphology for six-legged robots, by performing a systematic search of the leg morphology related parameters. Our aim is twofold: first, to gain an insight into the possible influence of leg morphology on the behaviors of six-legged robots, thereby extending our knowledge of leg morphology on legged systems; second, to choose a proper leg morphology for our developed six-leg robot (shown in Fig. 1a). This leg morphology is of particular importance, as it relates to the initiation and termination states and thus the overall locomotion of the robot. To the best of our knowledge, this is the first time to systematically investigate the respective roles of leg morphology in six-legged robots. In particular, we hope this paper could serve as a paradigmatic case study of leg morphology design and analysis for six-legged robots. The remainder of the paper is organized as follows: firstly, the investigated robot in this study is briefly introduced, the research problem to be solved is also systematically stated in this

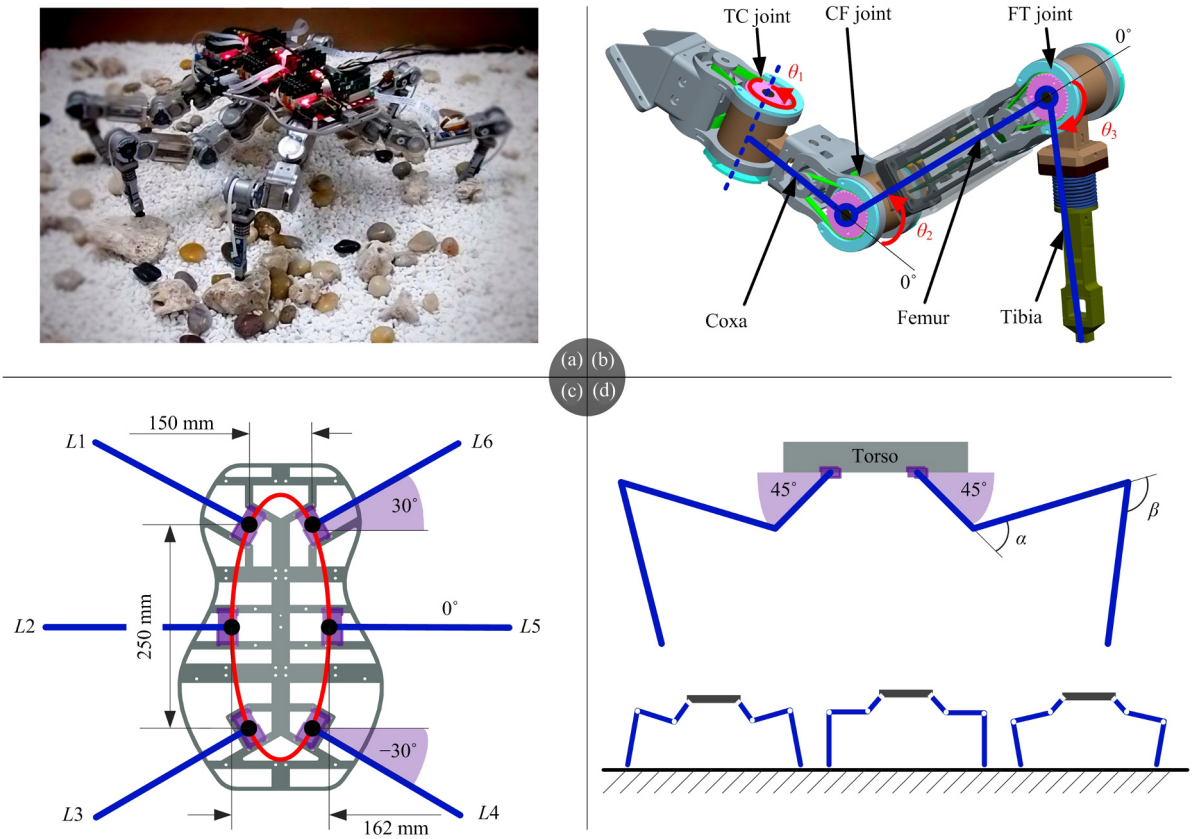

Fig. 1 The six-legged robot alongside its leg configurations. (a) Physical prototype of the robot; (b) leg design; (c) mounting locations and orientation of legs with respect to the torso; (d) illustration of various leg morphology determined by default angles α and β of femur and tibia joints.

section. Then behavioral changes of the robot with different leg morphology are compared and contrasted in detail from several points of view, followed by necessary interpretation to the observed behaviors. Finally, several issues with this study are discussed.

2 Robot and methods

This section describes the physical system of the six-legged robot, further states the problem to be addressed, and introduces the metrics by which the respective advantages and disadvantages of different leg morphology can be evaluated.

2.1 The six-legged robot and problem statement

The robot considered in this paper is depicted in Fig. 1. It consists of a torso manufactured in aluminum plate and six legs that are elliptically distributed around the torso (the corresponding mounting locations are illustrated in Fig. 1c). The six legs are designed identical for ease of manufacturing, maintenance, modelling and controlling. Each leg has three segments connected by joints, from proximal to distal: coxa, femur, tibia, as illustrated in Fig. 1b. Accordingly, the three revolute joints in each leg are, proximal to distal: Torso-Coxa (TC) joint for protraction and retraction, Coxa-Femur (CF) joint for elevation and depression, and Femur-Tibia (FT) joint for extension and flexion. The joints are powered by brushless DC servomotors each combined with a synchronous belt drive and a harmonic drive for speed reduction and torque amplification. Control system of the robot consists of a host computer for giving motion tasks, an ARM and DSP based main controller for motion planning, and six DSP based leg controllers for generating leg movements and controlling the motors. The relevant parameter set of the robot is displayed in Table 1. Additional details are available in Refs. [13] and [20].

In terms of the mounting orientation of legs relative to the torso, two structure parameters are involved. The first is the angle of each leg relative to the vertical axis, called mounting steering angle Ψ_S. From front to rear legs, mounting steering angle is 30°, 0°, −30°, respectively, as illustrated in Fig. 1c. Such setting is to reduce the possibility of inter-leg interference and improve walking stability. The other structure parameter is the angle of each leg relative to the horizontal plane, called mounting tilt angle Ψ_T. Mounting tilt angle for this robot is 45° (see Fig. 1d).

Table 1 Robot parameters

Symbol	Description	Value/Range
	Constant parameters	
M	Robot mass	3.26 kg
l_1	Length of coxa segment	48 mm
l_2	Length of femur segment	140 mm
l_3	Length of tibia segment	122 mm
Ψ_T	Mounting tilt angle of legs relative to the horizontal plane	45°
Ψ_S	Mounting steering angle of legs relative to the vertical axis	Front: 30° Middle: 0° Rear: −30°
	Variable parameters	
θ_1	Angle of coxa joint	[−45°, 45°]
θ_2	Angle of femur joint	[30°, 75°]
θ_3	Angle of tibia joint	[30°, 120°]
	Investigated parameters	
α	Default angle of femur joint	–
β	Default angle of tibia joint	–

As animals have different leg morphology, various options of leg morphology exist with the six-legged robot in this study, characterized by CF joint angle α and FT joint angle β, as illustrated in Fig. 1d. As representative examples, Fig. 1d displays three typical options of leg morphology. Such leg morphology has a great influence on the kinematic flexibility of legs and torso and even the dynamics during locomotion. From this perspective, the aim of this study is to, by scanning over the parameter space formed by α and β, systematically examine the respective advantages and disadvantages of different leg morphology and provide guidelines for rationally designing the leg morphology of six-legged robots.

2.2 Performance metrics

One of the key issues in this paper is to determine which aspects of performance to focus on. There have been various behavioral performances investigated for legged robots, and it is crucial to judiciously single out those most important for the robot discussed. It is noteworthy that even the similar type of robots may focus on different aspects of performance, heavily depending on the design purposes and application scenarios of the robots. In this paper, the six-legged robot is expected to be employed in some scenarios with rugged

$$\boldsymbol{J}=\begin{bmatrix} -c\psi_T s_1\left(l_1+l_2c_2+l_3c_{23}\right) & -c\psi_T c_1\left(l_2s_2+l_3s_{23}\right)+s\psi_T\left(l_2c_2+l_3c_{23}\right) & -c\psi_T c_1 l_3 s_{23}+s\psi_T l_3 c_{23} \\ c_1\left(l_1+l_2c_2+l_3c_{23}\right) & -s_1\left(l_2s_2+l_3s_{23}\right) & -s_1 l_3 s_{23} \\ s\psi_T s_1\left(l_1+l_2c_2+l_3c_{23}\right) & s\psi_T c_1\left(l_2s_2+l_3s_{23}\right)+c\psi_T\left(l_2c_2+l_3c_{23}\right) & s\psi_T c_1 l_3 s_{23}+c\psi_T l_3 c_{23} \end{bmatrix}. \tag{1}$$

$$w=\sqrt{\left|\boldsymbol{J}\boldsymbol{J}^{\mathrm{T}}\right|}=\sigma_1\sigma_2\sigma_3= \frac{l_2l_3}{2}\sqrt{\left[1-c\left(2\theta_3\right)\right]}\left\{l_2^2\left[c\left(2\theta_2\right)+1\right]+l_3^2\left[c\left(2\theta_2+2\theta_3\right)+1\right]+2l_1^2+4l_1\left(l_2c_2+l_3c_{23}\right)+2l_2l_3\left[c_3+c\left(2\theta_2+\theta_3\right)\right]\right\}^{1/2}. \tag{2}$$

terrain and a stereo camera head would be placed on the torso to perceive its surrounding environment. As a correspondence, the relative role of leg morphology will be evaluated from two aspects, each using two performance metrics, namely (I) leg kinematic flexibility, (II) torso kinematic flexibility, (III) walking energy efficiency, (IV) walking rolling stability.

2.2.1 Metric I: leg kinematic flexibility

Leg kinematic flexibility is essential for the omnidirectional mobility of the six-legged robot over rugged terrains. It has a remarkable influence on the maximum step sizes and maximum obstacle height the robot can walk over. In addition, owing to the redundancy resulting from multiple legs, it is also possible to manipulate objects with some of the legs. For the purpose of characterizing the kinematic flexibility of a leg at a certain morphology, the measure of manipulability proposed by Yoshikawa is used in this paper[21]. This measure can quantify the moving capacity of legs in positioning and orienting their foot tips. According to the definition, the manipulability can be calculated through the Jacobian matrix $\boldsymbol{J}$. In specific, the Jacobian matrix of the six-legged robot leg is presented in Eq. (1). In Eq. (1), Ψ_T is the mounting tilt angle of legs relative to the horizontal plane; c and s mean cosine and sine functions; and s_{123} and c_{123} stand for $\sin(\theta_1+\theta_2+\theta_3)$ and $\cos(\theta_1+\theta_2+\theta_3)$, respectively. Therefore, the manipulability can be calculated by Eq. (2). In Eq. (2), σ_1, σ_2, σ_3 are singular values of the Jacobian matrix $\boldsymbol{J}$.

In addition, for simplicity of description, the manipulability can be illustrated as manipulability ellipsoid whose principle axes are constituted by σ_1, σ_2, σ_3. In such a setting, volume of the ellipsoid is directly proportional to the manipulability. In the following analysis, we will use the ellipsoid volume to characterize leg kinematic flexibility.

2.2.2 Metric II: torso kinematic flexibility

During walking of the six-legged robot, the torso is normally supported by those legs on the ground. The capability of adjusting the position and orientation of the robot torso is beneficial to homogenize foot forces as well as improving traversability (*i.e.* the ability to overcome rough terrains). More importantly, the torso essentially plays the role of a floating base on which the legs in the air are attached. The reachable area of these swing legs can be expanded by appropriately moving the torso, which is extremely important in challenging terrains where possible footholds are relatively sparse since it can help legs reach further and probably more effective footholds.

Generally, the torso pose in the ground reference frame is given by a 6-dimensional vector, consisting of a 3-dimensional vector describing the position of the Center of Mass (CoM) of the torso and a 3-dimensional vector describing the orientation of the torso with respect to the reference frame. To the best of our knowledge, quantifying the kinematic flexibility of such a 6-dimensional vector is a tricky business. Inspired by the techniques of parallel manipulators, in this paper we define the torso kinematic flexibility by simply calculating the volume of the torso kinematic workspace for a constant orientation (0, 0, 0)[22,23]. As we are only interested in choosing the parameters with larger reachable range by comparison across different leg morphology.

In order to calculate torso workspace volume, the boundary search method is used in this paper[24,25]. Specifically, as depicted in Fig. 2, we first search the boundary of the workspace in the xy plane for every height z and calculate the corresponding area at this height, then approximate the workspace volume using

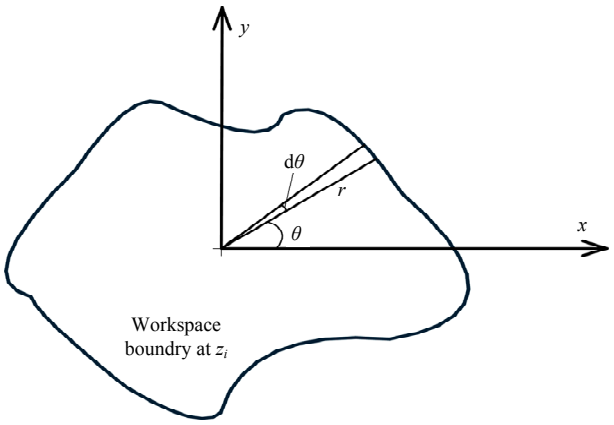

Fig. 2 Illustration of the boundary search method.

discrete integration over z. The specific steps adopted in the calculation of the workspace volume can be summarized in the following steps:

Step 1: Discretization of z values of the workspace volume from z_0 to z_1 with a step dz.

Step 2: For the plane denoted in polar coordinates at height z_i, search the maximum radial coordinate r within the workspace volume of the angular coordinate θ, by performing inverse kinematics to see if the point (r, θ) satisfies the allowable motion range of each leg joint. After every angular coordinate $\theta \in [0, 2\pi]$ is checked, the boundary of the volume at height z_i is found.

Step 3: Calculation of the area A_i at height z_i as follows:

$$A_i = \int_0^{2\pi} \frac{1}{2} r^2 \mathrm{d}\theta. \tag{3}$$

Step 4: Approximation the workspace volume using discrete integration over z.

$$V = \sum_{z_0}^{z_1} A_i \mathrm{d}z. \tag{4}$$

2.2.3 Metric III: walking energy efficiency

Energy efficiency is one of the primary considerations in legged locomotion, both for animals and robots[26–30]. Plenty of research has argued that biological systems shape their body and ways of locomotion for the sake of minimizing energetic cost[31–33]. For autonomous mobile machines, energy efficiency also determines to a large extent their autonomy, through imposing a limit on the distance and speed robots can go. Here, we use the mechanical energy consumed in each joint during walking to evaluate the energetic influence of leg morphology.

Several energy consumption models have been developed for legged robots with different actuating means[34]. However, according to our preliminary experiments and tests for electrical motor based consumption models, we found they are not accurate enough to measure the energy consumption for our six-legged robot as shown in Fig. 1a. The major reason is that mechanical loss such as friction in the transmission system of robotic joints cannot be ignored for the robot with small size and as many as 18 joints. Also, in this context, respective effects of the metric would be likely less marked or even eliminated if the mechanical loss is not properly estimated. With this fact in mind, instead of using theoretical calculations, the walking energy efficiency here are discussed with the real-world robot experiments, that is, the consumed mechanical energy of the robot can be approximated as follows:

$$E = \sum_{i=1}^{18} \int \left| \tau^i \right| \cdot \mathrm{d}\theta^i, \tag{5}$$

where τ^i denotes the measured torque sequence for joint i, θ^i represents the corresponding angular displacement.

A six-legged robot can perform a variety of gaits featuring very different properties. It is well known that alternating tripod gait is the fastest and most commonly used gait for six-legged walking. Thus, we focus our study on alternating-tripod gait. The similar simplification has also been taken in other related studies[34–37].

2.2.4 Metric IV: walking rolling stability

The fourth metric to be investigated is the extent of rolling oscillation with the torso during walking, referred as walking rolling stability. Rolling stability has been an important concern in legged locomotion in the last two decades[38,39]. It is particularly crucial for the systems concerning torso steadiness, for example, for those carrying laser or vision sensors to map unknown terrains. During normal walking with the six-legged robot, it is experimentally observed that the torso is accompanied by a certain degree of steady-state rolling oscillation. Torso rolling oscillation would add more noise into the sensors and is therefore thought to be undesirable. In this paper, we use maximum oscillating

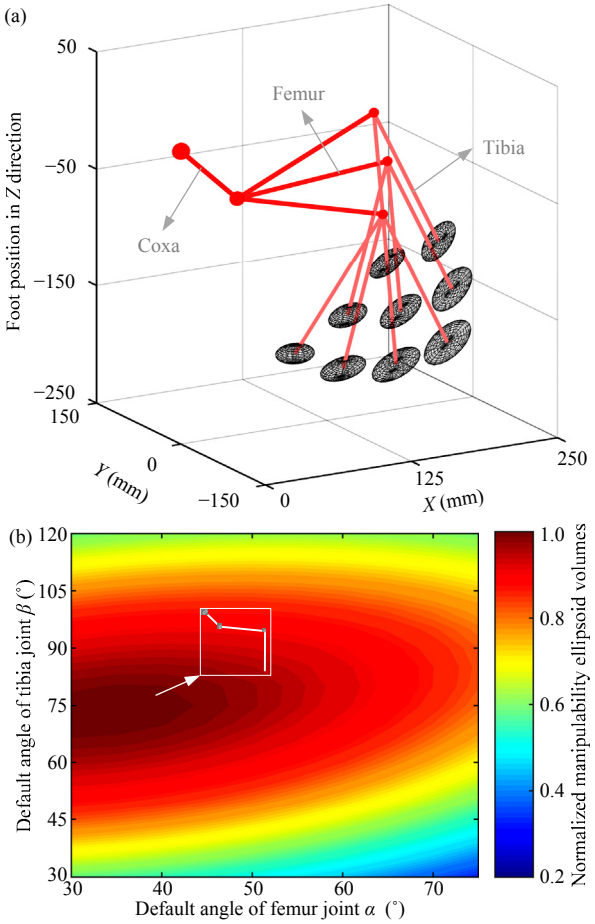

Fig. 3 Effect of leg morphology on leg kinematic flexibility. (a) Manipulability ellipsoids for several possible leg morphology; (b) normalized manipulability ellipsoid volumes against default angles of femur and tibia joints.

angle of the measured rolling motion as an index to characterize the rolling stability, namely

$$R = \max(r(\theta)), \tag{6}$$

where R is the maximum rolling angle used as the index, $r(\theta)$ denotes the experimentally recorded rolling motion.

3 Results

3.1 Effect of leg morphology on leg kinematic flexibility

Fig. 3a considers three groups of leg morphology (each group containing 2 – 4 kinds as representative examples), with manipulability ellipsoids illustrated at the foot end to characterize the corresponding leg kinematic flexibility. It is clearly seen that leg morphology greatly influences the manipulability performance, even though with the same dimensional parameters, underscoring the importance of leg morphology for leg kinematic flexibility.

A contour plot of manipulability ellipsoid volumes with respect to various leg morphology which are determined by default angles of femur and tibia joints are shown in Fig. 3b. To provide an intuitive comparison, we divided ellipsoid volume by the biggest one, so that we have a set of normalized manipulability ellipsoid volumes that range from 0 to 1. From this figure, it is apparent that the bigger ellipsoid volumes appear in the region formed by $\alpha \approx 30^\circ - 40^\circ$ and $\beta \approx 67^\circ - 77^\circ$, corresponding to the leg morphology where femur segment tilts downwards by $5^\circ - 10^\circ$ and where tibia segment is vertically downwards or with a slight outward/inward tilt. For the six-legged walking robot, such leg morphology results in a large torso height and thereby a relatively broad vertical range to lift up swing feet, which is advantageous for the robot to walk over high obstacles. In addition, during simulations, we noted that the manipulability ellipsoid volume changes little with the angle of coxa joint, indicating that coxa joint is probably not related to leg manipulability. This result can be explained analytically by the Eq. (2) in which there is no influence of θ_1.

3.2 Effect of leg morphology on torso kinematic flexibility

For an intuitive understanding of the influence of leg morphology on torso motion, Fig. 4 depicts the variations of torso workspace for four different leg morphologies. The four leg morphologies compared are ($\alpha = 45^\circ, \beta = 75^\circ$), ($\alpha = 45^\circ, \beta = 90^\circ$), ($\alpha = 60^\circ, \beta = 75^\circ$), and ($\alpha = 60^\circ, \beta = 90^\circ$). The transparent black flat surfaces in each subfigure correspond respectively to the maximum and minimum heights that the torso can reach with the specified leg morphology. It is apparent from this figure that leg morphology plays a direct role in the shape and contour of the torso workspace. Particularly, the specified leg morphology in essence sets a limit on the height range that the torso can move within as shown in the figure, which directly determines the maximum/minimum height the robot can walk over or get through.

The torso workspace volume is used to summarize the collective effect of leg morphology, whose variations

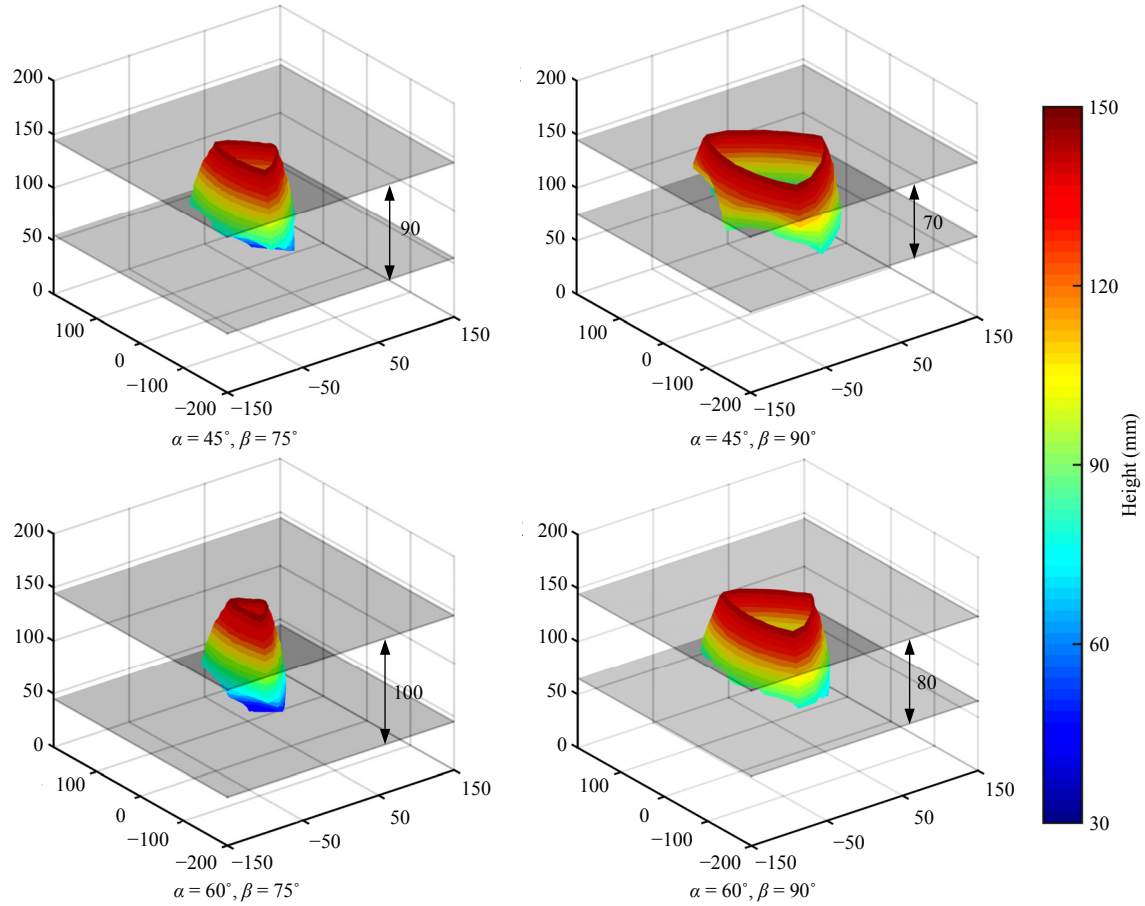

Fig. 4 Boundary contours of torso workspace for four groups of leg morphologies. The transparent black planes in each subfigure represent the largest and smallest heights that the torso can reach.

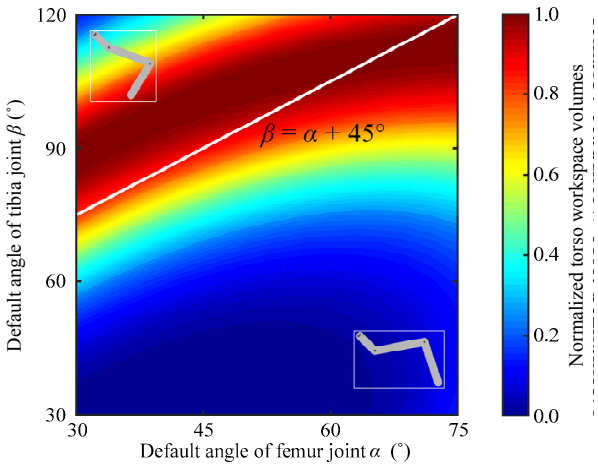

Fig. 5 Normalized torso workspace volumes against default angles of femur and tibia joints.

with respect to default angles of femur and tibia joints are depicted as a contour plot in Fig. 5. The two angle values are varied in the range of [30°, 75°] for α and [30°, 120°] for β. Likewise, each torso workspace volume is normalized to [0, 1], for the sake of comparison. The white line represents those leg morphology that tibia segment is vertically downwards, namely, $\beta = \alpha + 45°$. From this figure, perhaps the most striking observation is that there exists a narrow band close to the white line in which relatively better torso kinematic flexibility is achieved. One potential reason is that, with such leg morphology, the torso holds relatively broad motion range both in vertical and horizontal directions. Furthermore, it seems that β plays a much more decisive role than α in terms of torso workspace volume, as the volume values only have a slight change when fixing β and varying α.

3.3 Effect on walking energy efficiency and rolling stability

The results of mechanical energy consumed with 16 types of leg morphology are displayed as a scatter plot in Fig. 6. In order to increase the reliability of data, the walking trials for each leg morphology were repeated

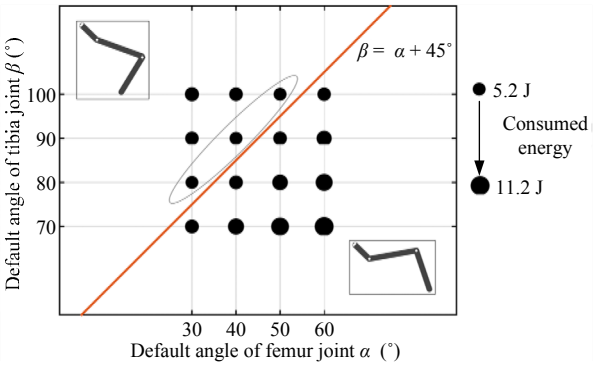

Fig. 6 Energy use during normal walking for different leg morphology determined by default angles of femur and tibia joints. Amounts of consumed mechanical energy are illustrated by sizes of the points.

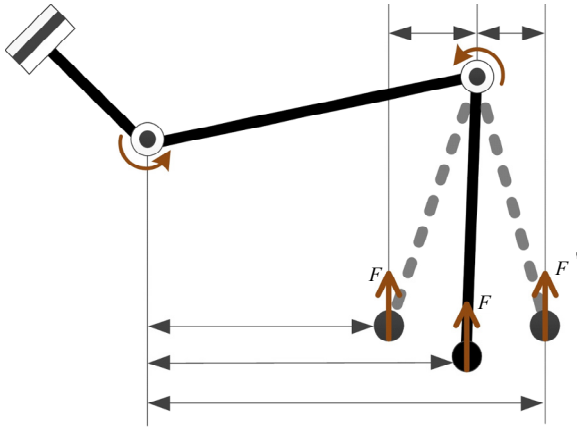

Fig. 7 Diagram of moment arms of ground reaction force F with respect to femur and tibia joints for different scenarios of leg morphology.

five times. The points in the figure are additionally size coded according to the standard deviation of the measured energy from 5.2J to 11.2J. The red line represents those leg morphology that tibia segment is vertically downwards, namely, $\beta = \alpha + 45°$. As a result, the upper and lower regions separated by the red line correspond to the situations where tibia segment tilts inwards and outwards, respectively. From this figure, it is apparent that the robot walks most efficiently with that leg morphology close to and located slightly at the upper part of the red line. And, an energy penalty is seen for leg morphology either side of the red line. By examining the variations of joint torque and angles that determine the mechanical energy, we found that a major factor leading to such results is perhaps those energy consumed to support the torso while walking. As schematically illustrated in Fig. 7, F denotes the ground reaction force with

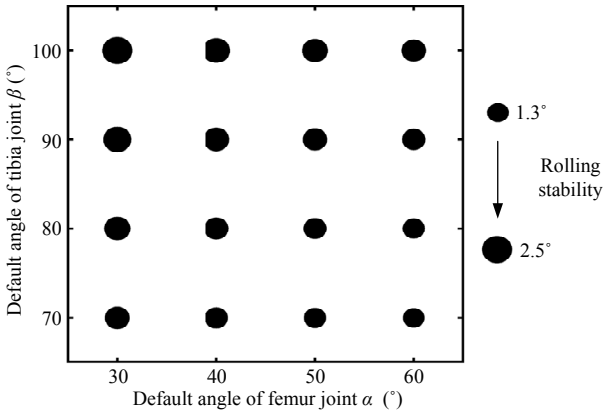

Fig. 8 Rolling stability during normal walking for different leg morphology. The maximum rolling angles are illustrated by sizes of the points.

one of the support legs, different scenarios of leg morphology correspond to different moment arms of F with respect to femur and tibia joints and thus different moments. Obviously, the scenario that tibia segment is vertically downwards or tilts a less degree inwards leads to a shorter moment arm with respect to femur joint as well as an almost zero moment arm with respect to tibia joint, meaning that less motor torque is needed to balance the moment of F.

The scatter plot in Fig. 8 gives the variations of rolling stability as a function of default angles of femur and tibia joints, with the points size coded for purposes of rolling stability indication analogously to the walking energy presented in Fig. 6. This figure indicates that rolling stability can be improved via increasing α and decreasing β, for the walking trials we considered, the improvement is from 2.5° with ($\alpha = 30°, \beta = 100°$) to 1.3° with ($\alpha = 60°, \beta = 70°$). From this observation, it can be reasonably inferred that a wider supporting polygon (decreasing β) and a low torso height (increasing α) are preferred to overcome rolling oscillations.

4 Discussion

This paper has presented a study of how leg morphology can influence the kinematic flexibility and walking behaviors of a six-legged robot. Our results showed leg morphology with the tibia segment vertically downwards is preferred for all the four metrics. However, a trade-off is observed for the femur segment: the femur segment should tilt downwards from kinematic flexibility point of view, while tilting upwards for energy-

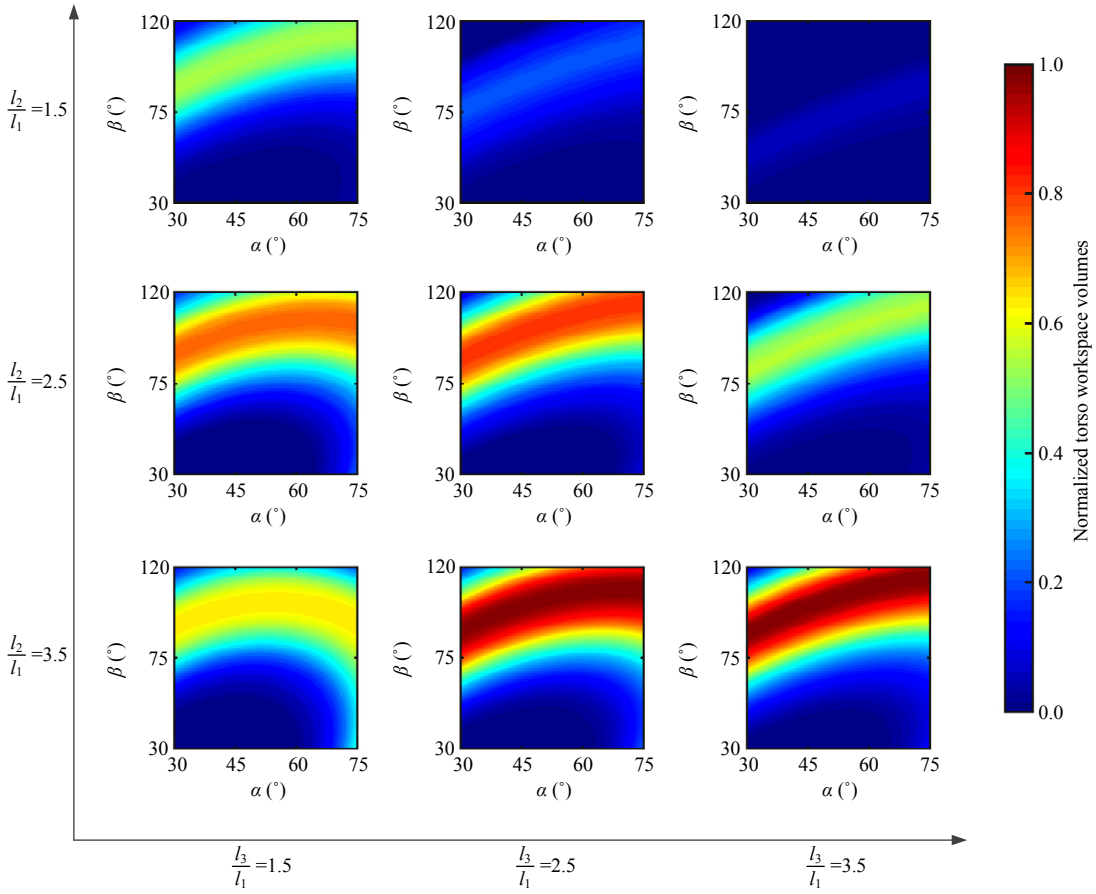

Fig. 9 Variations of torso kinematic flexibility for different proportions of leg segments.

efficient and steady walking. In this regard, the setting of the femur segment is dependent on the terrain conditions the robot is walking over. Specifically, our fundamental goal is to make sure the robot can traverse the given terrain with a suitable leg morphology. Therefore, if the terrain is challenging, for example, where effective footholds are relatively sparse and of high obstacle density, the kinematic flexibility performance would be prior, the femur segment should tilt downwards. In contrast, if the terrain is flat or slightly irregular, the femur segment should tilt upwards to achieve more energy-efficient and steady walking.

To the best of our knowledge, this is the first time to systematically investigate the respective roles of leg morphology in robots with six legs, extending our knowledge of leg morphology on legged systems. Moreover, such investigations could have important implications related to the construction of more structurally flexible and reasonable six-legged robots. In particular, we hope this paper could serve as a paradigmatic case study of leg morphology design and analysis for six-legged robots. To further facilitate our understanding, the following issues will be discussed.

4.1 On the influence of leg segment proportions

Most existing six-legged robots adopt similar three-segmented legs, but the relative proportions of leg segments differ from robot to robot[40–42]. In the previous investigations, lengths of the three leg segments are defined according to the specific size of the six-legged robot depicted in Fig. 1, that is, 48 mm, 140 mm and 122 mm, respectively.

Aiming to capture the influence of leg segment proportions on leg morphology design, we conducted a series of auxiliary simulation runs by varying the length of femur segment l_2 and the length of tibia segment l_3 in the range of $[1.5l_1, 3.5l_1]$ with a step of l_1 (l_1 represents the length of coxa segment), while keeping total length of the leg constant (310 mm). Fig. 9 depicts the variations of torso workspace for nine different proportions of

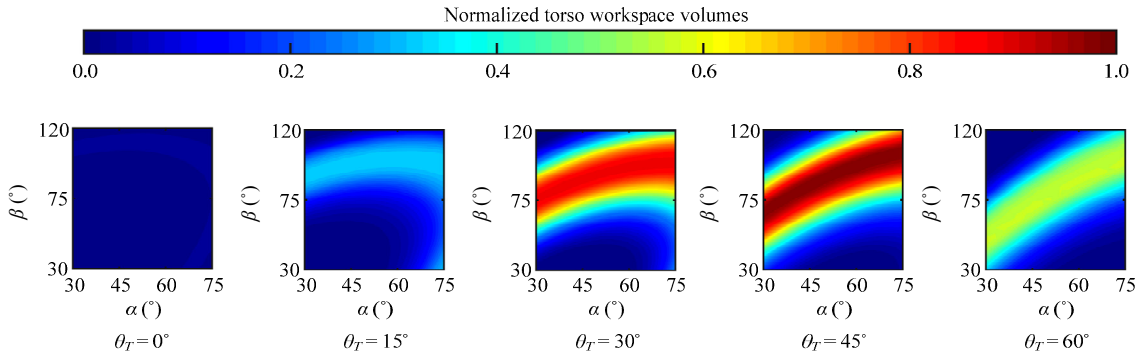

Fig. 10 Variations of torso kinematic flexibility for different mounting tilt angles.

leg segments. It can be observed that for each leg segment proportion, the tendencies of torso workspace volume relative to α and β are similar, with a narrow band existing in which relatively better torso kinematic flexibility is achieved. Such tendencies indicate that the variations of relative proportions of leg segments probably do not influence the results of leg morphology, from the angle of torso kinematic flexibility. Furthermore, by comparison with the best flexibility in each subfigure, it is speculated that advantageous proportions of leg segment lengths are $l_2 \approx 3.5l_1$ and $l_3 = (2.5 - 3.5)l_1$. Noted that due to the limited samples discussed, systematic investigations are still required to draw a more meaningful conclusion.

4.2 On the influence of leg mounting orientation relative to torso

Leg mounting orientation consisting of mounting steering angle Ψ_S and mounting tilt angle Ψ_T (see section **2.1**) is another crucial fact to be examined further. Here, our particular focus is placed on the mounting tilt angle Ψ_T, since Ψ_T is closely related to torso height and thereby torso movements. As an auxiliary study, five mounting tilt angles were pre-selected and analyzed, that is, $\Psi_T = [0^\circ, 15^\circ, 30^\circ, 45^\circ, 60^\circ]$.

Fig. 10 illustrates the corresponding torso workspace volumes for each Ψ_T, to indicate the change of torso kinematic flexibility. Similarly, the two joints are varied in the range of $[30^\circ, 75^\circ]$ for α and $[30^\circ, 120^\circ]$ for β. As can be seen from the figure that the mounting angle $\Psi_T = 45^\circ$ holds the best torso flexibility, and that a flexibility penalty is seen for those angle values either side of 45°. In particular, the angle $\Psi_T = 0^\circ$ shows the worst torso flexibility, mainly because of limited motion range with the torso in the vertical direction, suggesting that it is better to tilt the mounting orientation, that is, $\Psi_T > 0^\circ$. Systematic investigations on mounting orientation of the legs are still required and will be conducted in our following work.

4.3 Limitations and issues to be further explored

Through examining the role of leg morphology from several points of view, it becomes evident that, for a six-legged robot with specific kinematic structure, there should be a reasonable leg morphology that maximizes its locomotive ability and behavior. This clearly illustrates the necessity of our study. The particular focus of this work is on the leg morphology of a six-legged robot determined by default angles of each joint. In implementation of the study, the six legs are set to elliptically distribute relative to the torso. Such a setting has no influence on the analysis of a single leg, but obviously plays a role in characterizing torso flexibility and rolling stability, thus limiting the results to be extended to other robots with six legs. Also, as mentioned, lengths of each leg segment, which are key parameters to be further optimized, are given according to our developed robot platform. Therefore, a dimensional synthesis is required to be conducted by performing a global parametric study, including leg mounting positions and orientation relative to the torso, lengths of legs and each segment. In particular, optimization and statistics will be used to generalize the results beyond a particular system.

When experimentally investigating walking energy efficiency and rolling stability of the robot, our primary aim is to explore how various leg morphology could improve walking performance of the robot. Thus, in implementation of the study, we let the robot locomote

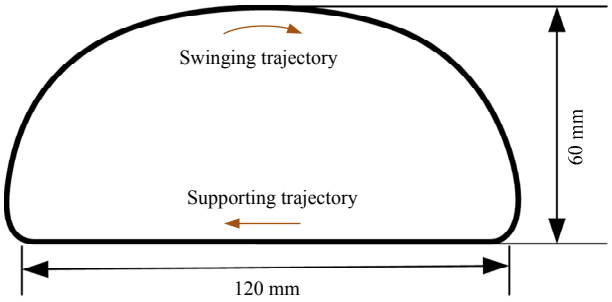

Fig. 11 Foot trajectories adapted during real-world experiments.

with the same foot trajectories (illustrated in Fig. 11) while varying leg morphology to produce a fair comparison of walking energy efficiency and rolling stability. This is a constraint we imposed for the experimental purpose. As a result, the robot may not locomote in the optimal way for each leg morphology. However, the walking performance can be potentially improved when more specific optimization processes can be implemented to explore the optimal parameter sets for a specific leg morphology. For example, the optimization can be implemented at one specific leg morphology, which takes into account the moving ways such as the stride frequency and the stride height of legs to efficiently exploit the robot's mechanical dynamics.

Regarding the third metric used in this study, walking energy efficiency, only the consumed mechanical energy is considered, aiming to quantitatively explore the influence of leg morphology on robot walking dynamics. In reality, in addition to mechanical consumption, some more energy is required to power the electronics like sensory and computational components, and there also exist a certain frictional and thermal electrical losses. Kinematic flexibility of torso is simply approximated by size of the torso position workspace, without thinking about the orientation variations. Therefore, a proper performance index to more precisely describe torso flexibility is required.

No passivity is included in our robotic platform. Plenty of research has pointed out that integrating passive elements into robotic structures could enhance their dynamic behaviors. Currently, we have conducted a theoretical study and revealed that stiffening passive compliance in parallel to joint is able to achieve a good tradeoff between energy efficiency and disturbance rejection[6]. In the future work, we will attempt to add such compliant elements into the six-legged robot.

5 Conclusion

In this work, the effects of leg morphology on the kinematic flexibility and walking performance of a six-legged robot are explored. Our results indicate that the leg morphology with femur segment tilting downwards and tibia segment vertically downwards or with a slight inward tilt is beneficial in terms of high kinematic flexibility. From the angle of robot locomoting, the leg morphology with femur segment tilting upwards and tibia segment approximately vertically downwards is more advantageous to achieve relatively energy-efficient and steady walking. Besides, several lessons can be learned from this study. First, careful mechanical design choices are able to passively enhance the behaviors of legged robots, which is particularly promising to reduce the burden of active control. Second, one certain leg morphology may exert contradictory influences on behaviors of the robot, as a result, necessary trade-offs have to be made. At a deeper level, the difference of leg morphology exhibited by animals with similar anatomical structures is probably evolved as the result of a trade-off between multiple desired behaviors, among which kinematic flexibility and walking performance might be two contributing factors.

Acknowledgement

This work was supported by Natural Science Foundation of China (Grant Nos. 51805074, U1713201 and 51605082), State Key Laboratory of Robotics and System (HIT) (Grant Nos. SKLRS-2018-KF-02 and SKLRS-2017-KF-07), China Postdoctoral Science Foundation (Grant Nos. 2018M631799 and 2019T120213), Fundamental Research Funds for the Central Universities (Grant Nos. N170303007 and N180304015) and Postdoctoral Science Foundation of Northeastern University (Grant No. 20180311).

References

[1] Liu Q Y, Chen X D, Han B, Luo Z W, Luo X. Learning control of quadruped robot galloping. *Journal of Bionic Engineering*, 2018, **15**, 329–640.

[2] Liu C J, Xu T, Wang D W, Chen Q J. Active balance of humanoids with foot positioning compensation and

non-parametric adaptation. *Robotics and Autonomous Systems*, 2016, **75**, 297–309.

[3] Zhang Z Q, Zhao J, Chen H L, Chen D S. A survey of bio-inspired jumping robot: Takeoff, air posture adjustment, and landing buffer. *Applied Bionics and Biomechanics*, 2017, **2017**, 4780160.

[4] Kwak B, Bae J. Locomotion of arthropods in aquatic environment and their applications in robotics. *Bioinspiration & Biomimetics*, 2018, **13**, 041002.

[5] Zhu H B, Luo M Z, Mei T, Zhao J H, Li T, Guo F Y. Energy-efficient bio-inspired gait planning and control for biped robot based on human locomotion analysis. *Journal of Bionic Engineering*, 2016, **13**, 271–282.

[6] Zhou X D, Bi S S. A survey of bio-inspired compliant legged robot designs. *Bioinspiration & Biomimetics*, 2012, **7**, 041001.

[7] Hutter M, Remy C D, Hoepflinger M A, Siegwart R. Efficient and versatile locomotion with highly compliant legs. *IEEE/ASME Transactions on Mechatronics*, 2013, **18**, 449–458.

[8] Chen D L, Li N J, Liu G F, Chen L, Wang Y Y, Liu C, Zhuang B. Effects of spine motion on foot slip in quadruped bounding. *Applied Bionics and Biomechanics*, 2018, **2018**, 8097371.

[9] Chen J, Jin H Z, Iida F, Zhao J. A design concept of parallel elasticity extracted from biological muscles for engineered actuators. *Bioinspiration & Biomimetics*, 2016, **11**, 056009.

[10] Haberland M, Kim S. On extracting design principles from biology: II. case study — The effect of knee direction on bipedal robot running efficiency. *Bioinspiration & biomimetics*, 2015, **10**, 016011.

[11] Daley M A, Channon A J, Nolan G S, Hall J. Preferred gait and walk-run transition speeds in ostriches measured using GPS-IMU sensors. *The Journal of Experimental Biology*, 2016, **219**, 3301–3308.

[12] Rubenson J, Lloyd D G, Heliams D B, Besier T F, Fournier P A. Adaptations for economical bipedal running: The effect of limb structure on three-dimensional joint mechanics. *Journal of the Royal Society Interface*, 2011, **8**, 740–755.

[13] Chen J, Liu Y B, Zhao J, Zhang H, Jin H Z. Biomimetic design and optimal swing of a hexapod robot leg. *Journal of Bionic Engineering*, 2014, **11**, 26–35.

[14] Zhong G L, Chen L, Jiao Z D, Li J F, Deng H. Locomotion control and gait planning of a novel hexapod robot using biomimetic neurons. *IEEE Transactions on Control Systems Technology*, 2018, **26**, 624–636.

[15] Zhao Y, Chai X, Gao F, Qi C K. Obstacle avoidance and motion planning scheme for a hexapod robot Octopus-III. *Robotics and Autonomous Systems*, 2018, **103**, 199–212.

[16] Smith J A, Jivraj J. Effect of hind leg morphology on performance of a canine-inspired quadrupedal robot. *Journal of Bionic Engineering*, 2015, **12**, 339–351.

[17] Semini C. *Hyq-Design and Development of a Hydraulically Actuated Quadruped Robot*, PhD thesis, University of Genoa, Genoa, Italy, 2010.

[18] Hutter M. *StarlETH & Co*: *Design and Control of Legged Robots with Compliant Actuation*, PhD thesis, Swiss Federal Institute of Technology Zurich, Zurich, Switzland, 2013.

[19] Lee D V, Meek S G. Directionally compliant legs influence the intrinsic pitch behaviour of a trotting quadruped. *Proceedings of the Royal Society B*: *Biological Sciences*, 2005, **272**, 567–572.

[20] Zhang H, Liu Y B, Zhao J, Chen J, Yan J H. Development of a bionic hexapod robot for walking on unstructured terrain. *Journal of Bionic Engineering*, 2014, **11**, 176–187.

[21] Yoshikawa T. Manipulability of robotic mechanisms. *The International Journal of Robotics Research*, 1985, **4**, 3–9.

[22] Cammarata A. Optimized design of a large-workspace 2-DOF parallel robot for solar tracking systems. *Mechanism and Machine Theory*, 2015, **83**, 175–186.

[23] Altuzarra O, Pinto C, Sandru B, Hernandez A. Optimal dimensioning for parallel manipulators: workspace, dexterity, and energy. *Journal of Mechanical Design*, 2011, **133**, 041007.

[24] Wang Z, Wang Z X, Liu W T, Lei Y C. A study on workspace, boundary workspace analysis and workpiece positioning for parallel machine tools. *Mechanism and Machine Theory*, 2001, **36**, 605–622.

[25] Zhao J S, Chu F, Feng Z J. Symmetrical characteristics of the workspace for spatial parallel mechanisms with symmetric structure. *Mechanism and Machine Theory*, 2008, **43**, 427–444.

[26] Hector M, Lisbeth M, Roemi F, Manuel A. Energy-efficiency hexapod walking robot for humanitarian demining. *Industrial Robot*: *The International Journal of Robotics Research and Application*, 2017, **44**, 457–466.

[27] Collins S, Ruina A, Tedrake R, Wisse M, Efficient bipedal robots based on passive-dynamic walkers. *Science*, 2005, **307**, 1082–1085.

[28] Seok S, Wang A, Chuah M Y, Hyun D J, Lee J, Otten D M, Lang J H, Kim S. Design principles for energy-efficient legged locomotion and implementation on the MIT cheetah robot. *IEEE/ASME Transactions on Mechatronics*, 2015, **20**, 1117–1129.

[29] di Prampero P E. The energy cost of human locomotion on land and in water. *International Journal of Sports Medicine*, 1986, **7**, 55–72.

[30] Cherouvim N, Papadopoulos E. Energy saving passive-dynamic gait for a one-legged hopping robot. *Robotica*, 2006, **24**, 491–498.

[31] Xi W T, Yevgeniy Y, Remy C D. Selecting gaits for economical locomotion of legged robots. *The International Journal of Robotics Research*, 2015, **35**, 1140–1154.

[32] Hoyt D F, Taylor C R. Gait and the energetics of locomotion in horses. *Nature*, 1981, **292**, 239.

[33] Umberger B R, Martin P E. Mechanical power and efficiency of level walking with different stride rates. *Journal of Experimental Biology*, 2007, **210**, 3255–3265.

[34] de Santos P G, Garcia E, Ponticelli R, Armada M. Minimizing energy consumption in hexapod robots. *Advanced Robotics*, 2009, **23**, 681–704.

[35] Sun Q, Gao F, Chen X B. Towards dynamic alternating tripod trotting of a pony-sized hexapod robot for disaster rescuing based on multi-modal impedance control. *Robotica*, 2018, **36**, 1048–1076.

[36] Bjelonic M, Kottege N, Homberger T, Borges P, Beckerle P, Chli M. Weaver: Hexapod robot for autonomous navigationon unstructured terrain. *Journal of Field Robotics*, 2018, **35**, 1063–1079.

[37] Dominik B, Przemyslaw L, Piotr S. Adaptive motion planning for autonomous rough terrain traversal with a walking robot. *Journal of Field Robotics*, 2016, **33**, 337–370.

[38] Rosendo A, Liu X X, Shimizu M, Hosoda K. Stretch reflex improves rolling stability during hopping of a decerebrate biped system. *Bioinspiration & Biomimetics*, 2015, **10**, 016008.

[39] Chatzakos P, Papadopoulos E. A parametric study on the rolling motion of dynamically running quadrupeds during pronking, *Proceedings of the* 17*th Mediterranean Conference on Control and Automation*, Thessaloniki, Greece, 2009, 754–759.

[40] Roy S S, Singh A K, Pratihar D K. Estimation of optimal feet forces and joint torques for on-line control of six-legged robot. *Robotics and Computer-Integrated Manufacturing*, 2011, **27**, 910–917.

[41] Wang Z Y, Ding X L, Rovetta A. Analysis of typical locomotion of a symmetric hexapod robot. *Robotica*, 2009, **28**, 893–907.

[42] Xu K, Ding X L. Typical gait analysis of a six-legged robot in the context of metamorphic mechanism theory. *Chinese Journal of Mechanical Engineering*, 2013, **26**, 771–783.